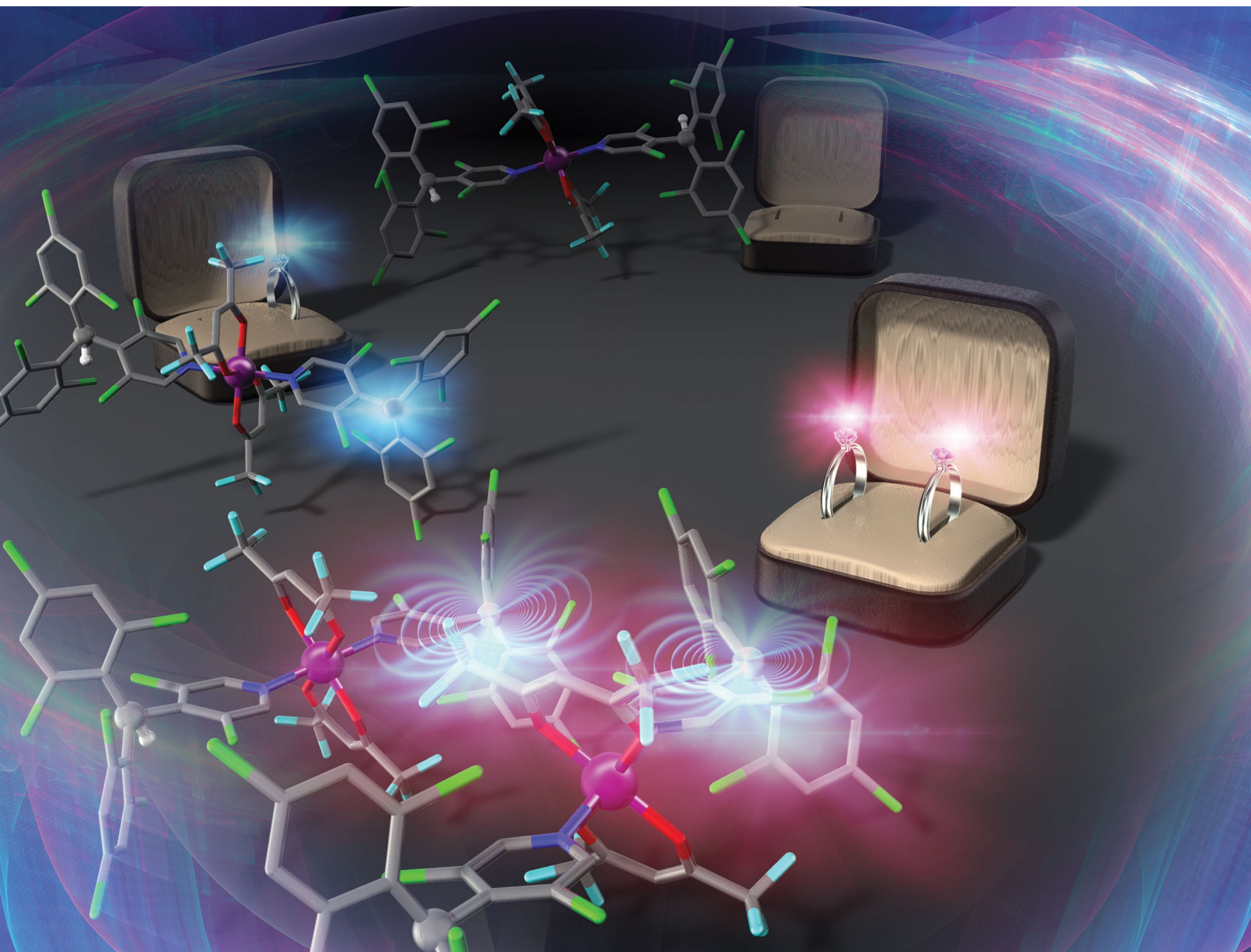


ChemComm

Chemical Communications

rsc.li/chemcomm



ISSN 1359-7345

COMMUNICATION

Hiroshi Nishihara, Tetsuro Kusamoto *et al.*
Excimer emission and magnetoluminescence of
radical-based zinc(II) complexes doped in host crystals



Cite this: *Chem. Commun.*, 2020, 56, 11195

Received 14th July 2020,
Accepted 21st August 2020

DOI: 10.1039/d0cc04830e

rsc.li/chemcomm

Excimer emission and magnetoluminescence of radical-based zinc(II) complexes doped in host crystals†

Shun Kimura,^{ab} Shojiro Kimura,^c Hiroshi Nishihara^{*bd} and Tetsuro Kusamoto^{ib} ^{★a}

A Zn^{II} complex based on a luminescent organic radical was doped into host molecular crystals. The 5, 10, and 20 wt%-doped crystals showed excimer emissions and their luminescent behaviours were significantly modulated by an external magnetic field. These are the first examples showing excimer emissions and magnetic-field-sensitive luminescent properties for complexes based on luminescent radicals. The excimer species contributing to magnetoluminescence was determined by analyzing the emission spectra and their magnetic-field dependencies. These results suggest the general nature of magnetic field effects on the luminescence of radicals as well as the importance of the type of interaction between radicals.

Luminescent organic molecules have been developed for wide-ranging applications, including organic light-emitting diodes (OLEDs)¹ and bioimaging.² Recently, luminescent radicals have attracted much attention^{3–6} because of their unusual characteristics, such as long-wavelength emissions, the absence of heavy-atom effect, and the high electron–photon conversion efficiency of OLEDs. These properties arise from the unique spin states of radical molecules with an unpaired electron, so that controlling the spin state is the key to new photochemical and photophysical properties, which are difficult to realize with conventional closed-shell luminophores. We recently reported that the (3,5-dichloro-4-pyridyl)bis(2,4,6-trichlorophenyl)methyl radical (PyBTM)^{6b} doped into (3,5-dichloro-4-pyridyl)bis(2,4,6-trichlorophenyl)methane (α H-PyBTM) molecular crystals^{7,8} exhibits a new luminescent property for organic radicals that stems from the interplay

between spin and luminescence. Crystals containing 10 wt% PyBTM displayed PyBTM monomer- and PyBTM excimer-centred emissions and magnetic-field-sensitive luminescence, namely, ‘magnetoluminescence’. These studies suggested that changes in spin multiplicities of aggregated radicals contributed to the magnetic-field effect (MFE). However, magnetoluminescence of stable radicals has to date been observed for only a few pure organic luminescent radicals. Therefore, the scope of candidate complexes showing magnetoluminescence should be expanded to provide new photofunctions in organic radicals. In particular, the development of metal–radical complexes that exhibit magnetoluminescence is a promising approach because of the ease of controlling the molecular and electronic structures through molecular design.

In this study, we prepared Zn^{II}(hfac)₂(α H-PyBTM)₂ (where hfac is hexafluoroacetylacetonato; Fig. 1a) crystals in which α H-PyBTM was substituted with PyBTM, and investigated their luminescent properties at different radical concentrations and under an applied magnetic field. The 5, 10, and 20 wt%-substituted crystals



Fig. 1 (a) Structures of Zn^{II}(hfac)₂(α H-PyBTM)₂, Zn^{II}(hfac)₂(α H-PyBTM)(PyBTM), and Zn^{II}(hfac)₂(PyBTM)₂. (b and c) Spin multiplicity changes in (b) Zn^{II}(hfac)₂(PyBTM)₂ and (c) Zn^{II}(hfac)₂(α H-PyBTM)(PyBTM) dimer.

^a Institute for Molecular Science, 5-1 Higashiyama, Myodaiji, Okazaki, Aichi 444-8787, Japan. E-mail: kusamoto@ims.ac.jp

^b Department of Chemistry, Graduate School of Science, The University of Tokyo, 7-3-1 Hongo, Bunkyo-ku, Tokyo, 113-0033, Japan

^c Institute for Materials Research, Tohoku University, 2-1-1 Katahira, Aoba-ku, Sendai, 980-8577, Japan

^d Research Center for Science and Technology, Tokyo University of Science, 2641 Yamazaki, Noda, Chiba 278-8510, Japan. E-mail: nishihara@rs.tus.ac.jp

† Electronic supplementary information (ESI) available: Experimental details and supplementary figures. CCDC 2008148. For ESI and crystallographic data in CIF or other electronic format see DOI: 10.1039/d0cc04830e

are the first reports of luminescent radical-coordinated metal complexes displaying excimer emissions. Their luminescent behaviours were modulated substantially by an external magnetic field, suggesting that magnetic-field-sensitive emission properties may be common, even in metal complexes with luminescent radicals. Two types of spin multiplicity changes, which would contribute to the MFE, were assumed to occur in this system: intramolecular changes in $\text{Zn}^{\text{II}}(\text{hfac})_2(\text{PyBTM})_2$ (Fig. 1b) and intermolecular changes in the $\text{Zn}^{\text{II}}(\text{hfac})_2(\alpha\text{H-PyBTM})(\text{PyBTM})$ dimer (Fig. 1c). Here we discuss which of these changes contributed to the magnetoluminescence.

$\text{Zn}^{\text{II}}(\text{hfac})_2(\alpha\text{H-PyBTM})_2$ was synthesized and characterized by the procedure described in the ESI†. A single-crystal X-ray diffraction study revealed the crystal structure of $\text{Zn}^{\text{II}}(\text{hfac})_2(\alpha\text{H-PyBTM})_2$ with the triclinic space group $P\bar{1}$ (Fig. 2). The unit cell contains two crystallographically independent $\text{Zn}^{\text{II}}(\text{hfac})_2(\alpha\text{H-PyBTM})_2$ molecules with almost identical structures. The $\text{Zn}^{\text{II}}(\text{hfac})_2(\alpha\text{H-PyBTM})_2$ crystals were isostructural with $\text{Zn}^{\text{II}}(\text{hfac})_2(\text{PyBTM})_2$ crystals⁹ except for the positions of the central carbon atoms of two (αH -PyBTMs), which were sp^3 -hybridized and disordered into two positions in the former crystals while sp^2 -hybridized in the latter. In one of the two crystallographically independent molecules, the trifluoromethyl groups in the hfac ligands were also disordered in two positions.

PyBTM-substituted $\text{Zn}^{\text{II}}(\text{hfac})_2(\alpha\text{H-PyBTM})_2$ with various PyBTM concentrations (1, 5, 10, and 20 wt% with respect to the sum of $\alpha\text{H-PyBTM}$ and PyBTM in the crystals) were prepared as follows. PyBTM, $\alpha\text{H-PyBTM}$, and $\text{Zn}^{\text{II}}(\text{hfac})_2$ were dissolved in dry dichloromethane. The solvent was allowed to evaporate slowly under dark and ambient conditions and the PyBTM-doped $\text{Zn}^{\text{II}}(\text{hfac})_2(\alpha\text{H-PyBTM})_2$ (**PyZn_R**, where *R* indicates the concentration (wt%) of PyBTM) crystals were washed with dry hexane. Powder X-ray diffraction (PXRD) revealed the uniformity of the crystal structures of **PyZn_R** (Fig. S3, ESI†). The PXRD patterns of **PyZn₁**, **PyZn₅**, **PyZn₁₀**, and **PyZn₂₀** were similar to those of $\text{Zn}^{\text{II}}(\text{hfac})_2(\alpha\text{H-PyBTM})_2$ and $\text{Zn}^{\text{II}}(\text{hfac})_2(\text{PyBTM})_2$.



Fig. 2 Crystal structure of $\text{Zn}^{\text{II}}(\text{hfac})_2(\alpha\text{H-PyBTM})_2$ viewed along the *a*-axis. Disorders of the trifluoromethyl groups and central carbon atoms of $\alpha\text{H-PyBTM}$ are omitted for clarity.

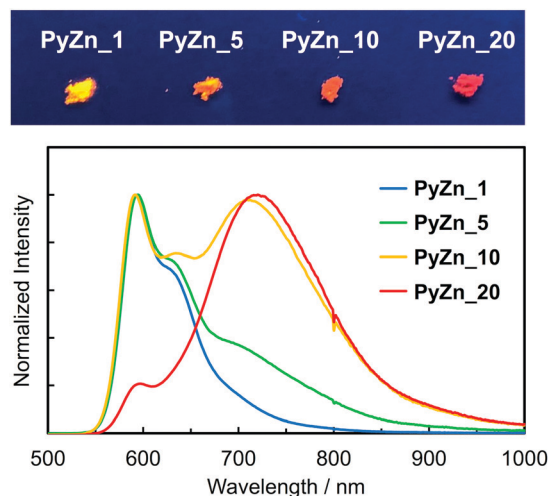


Fig. 3 Normalized emission spectra (lower, $\lambda_{\text{ex}} = 370$ nm) and image (upper, $\lambda_{\text{ex}} = 365$ nm) of **PyZn_R**.

These results suggest that $\alpha\text{H-PyBTM}$ was substituted for PyBTM while maintaining the original crystal structure. We assumed that the $\text{Zn}^{\text{II}}(\text{hfac})_2(\alpha\text{H-PyBTM})_2$, $\text{Zn}^{\text{II}}(\text{hfac})_2(\alpha\text{H-PyBTM})(\text{PyBTM})$, and $\text{Zn}^{\text{II}}(\text{hfac})_2(\text{PyBTM})_2$ species were randomly mixed in the crystals (Fig. 1a).

The luminescent behaviours of **PyZn_R** depended strongly on the radical concentration. **PyZn₁**, with the lowest radical concentration, had a maximum emission wavelength, λ_{em} , of 595 nm upon excitation at $\lambda_{\text{ex}} = 370$ nm (Fig. 3). Considering the low concentration of PyBTM, the emission was derived from $\text{Zn}^{\text{II}}(\text{hfac})_2(\alpha\text{H-PyBTM})(\text{PyBTM})$, the complex with coordinating one radical. This spectral shape was similar to that of 1 wt% PyBTM-doped $\alpha\text{H-PyBTM}$ ($\lambda_{\text{em}} = 563$ nm).⁷ This bathochromic shift in emission wavelength was caused by coordination to the positively charged zinc ion, as observed in the $\text{Au}^{\text{I}}\text{-PyBTM}$ complex; the coordination was expected to lower the energy level of the β -singly occupied molecular orbital, decreasing the emission energy.^{6b,c,10} As the radical concentration increased, a new emission band at around $\lambda_{\text{em}} = 725$ nm appeared and emission at 595 nm was suppressed. These trends are similar to those reported in the previous studies,^{7,11} and the new long-wavelength emission band was attributed to the excimer. The excimer character was confirmed by measuring the excitation spectra of **PyZn₁₀** at monomer- and excimer-centred emission maximum wavelengths ($\lambda_{\text{em}} = 595$ and 725 nm, respectively). These spectra were similar (Fig. S4, ESI†), suggesting that the long-wavelength emission was derived from the excimer formed after photoexcitation.¹² Although $\text{Zn}^{\text{II}}(\text{hfac})_2(\alpha\text{H-PyBTM})_2$ and the $\text{Zn}^{\text{II}}(\text{hfac})_2(\alpha\text{H-PyBTM})(\text{PyBTM})$ dimer were possible candidates for the excimer, the species from which the excimer emission originated could not be identified because they were randomly mixed throughout the samples. We could not obtain the emission spectrum of isolated $\text{Zn}^{\text{II}}(\text{hfac})_2(\text{PyBTM})_2$ because of the dissociation of PyBTM, which occurred in solution⁹ and during grinding with a solid matrix (Fig. S5, ESI†).

The photophysical properties of **PyZn_R** are summarized in Table S1 (ESI†). **PyZn₁** had the highest luminescent quantum

yield, ϕ_{em} , of 18%; as the radical concentration increased, the excimer emission appeared and the ϕ_{em} value of **PyZn_R** decreased to 5.2% for **PyZn_20**. This is explained by concentration quenching in the crystals, with the quantum yield of excimer emission being lower than that of monomer emission. The emission lifetime at the excimer-centred emission wavelengths for **PyZn_5**, **PyZn_10**, and **PyZn_20** was longer than that at the monomer-centred emission wavelengths and the emission decay could be fitted with a single exponential curve (Fig. S6, ESI†). This indicates that the excimer was a single component, and thus either $\text{Zn}^{\text{II}}(\text{hfac})_2(\alpha\text{H-PyBTM})_2$ or the $\text{Zn}^{\text{II}}(\text{hfac})_2(\alpha\text{H-PyBTM})(\text{PyBTM})$ dimer was emissive.

The emission spectra of **PyZn_R** under an external magnetic field at 4.2 K were measured to investigate the MFE on the luminescent behaviour. Fig. 4a shows the emission spectra of **PyZn_1**, which displayed only monomer-centred emission, under applied magnetic fields of 0, 5, 10, 15, and 18 T. The spectra were not affected by these magnetic fields, suggesting an absence of MFE. This is consistent with our previous report, in which isolated PyBTM did not show an MFE because of its luminescent character being based on a doublet-doublet transition.⁷ In contrast, the emissions of samples with higher radical concentrations, **PyZn_5**, **PyZn_10**, and **PyZn_20**, which displayed monomer- and excimer-centred emissions, were clearly modulated by an external magnetic field (Fig. 4b–d). As the applied magnetic field increased, the monomer-centred emission at $\lambda_{\text{em}} = 595$ nm was strongly enhanced and the excimer-centred emission at $\lambda_{\text{em}} = 740$ nm was slightly suppressed. This is the first-reported example of an MFE observed for luminescent metal complexes with a coordinated luminescent radical. Fig. 5a and Fig. S7 (ESI†) show the intensity changes at monomer and excimer emission wavelengths for **PyZn_5**, **PyZn_10**, and **PyZn_20**. Different emission spectra of **PyZn_10** are shown in Fig. 5b. The magnitudes of the intensity

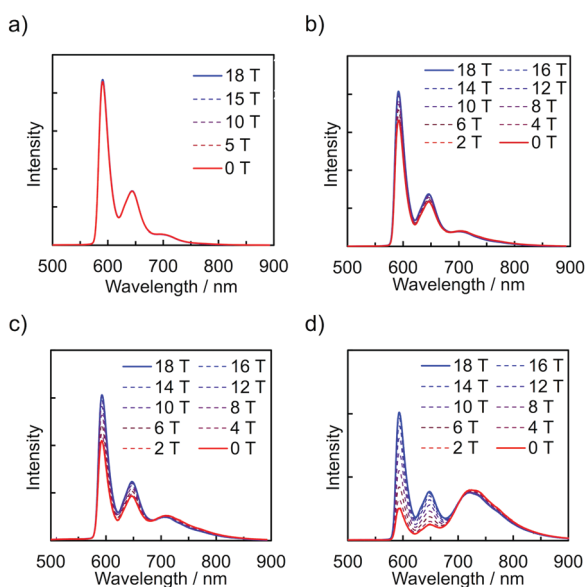


Fig. 4 Emission spectra of (a) **PyZn_1**, (b) **PyZn_5**, (c) **PyZn_10**, and (d) **PyZn_20** at 4.2 K under a magnetic field.



Fig. 5 (a) Intensity changes of **PyZn_10** at monomer ($\lambda_{\text{em}} = 595$ nm) and excimer ($\lambda_{\text{em}} = 740$ nm) emission wavelengths at 4.2 K under a magnetic field. Monomer enhancement and excimer suppression indicate the increase in monomer intensity and the decrease in excimer emission intensity from intensities at 0 T, respectively. (b) Difference emission spectra (Δ intensity) of **PyZn_10** at 4.2 K under magnetic fields compared with the spectrum under 0 T. (c) and (d) Emission spectra and the monomer and excimer emission components of (c) **PyZn_5** and (d) **PyZn_10**.

changes at the monomer- and excimer-centred emission wavelengths were related for each sample, and the increased monomer intensities were much larger than the decreased excimer emission intensities of **PyZn_5**, **PyZn_10**, and **PyZn_20** (21, 18, and 28 times, respectively). The monomer excited state thus had a much higher quantum yield than the excimer excited state.

In this system, $\text{Zn}^{\text{II}}(\text{hfac})_2(\text{PyBTM})_2$ and the $\text{Zn}^{\text{II}}(\text{hfac})_2(\alpha\text{H-PyBTM})(\text{PyBTM})$ dimer were both potential contributors to the excimer emissions and the magnetoluminescence. As suggested by the decay curves of the excimer emissions, which could be fitted with single components, the excimer emissive species was either one of the two species. To determine the excimer emissive species, the following three points were considered. First, the abundance ratio of $\text{Zn}^{\text{II}}(\text{hfac})_2(\text{PyBTM})_2$ was statistically much smaller than that of $\text{Zn}^{\text{II}}(\text{hfac})_2(\alpha\text{H-PyBTM})(\text{PyBTM})$ in the crystals of **PyZn_5** and **PyZn_10** (1/38 and 1/18, respectively). Second, the MFE on the emission spectra suggest that the emission quantum yield of the monomer excited state was much higher than that of the excimer excited state (Fig. 5a and Fig. S7, ESI†). Third, the contribution of excimer emission (I_{exc}) was comparable to that of the monomer emission (I_{mono}) in **PyZn_5** and **PyZn_10** ($I_{\text{mono}}:I_{\text{exc}} = 2.4:1.0$ and $0.6:1.0$, respectively; Fig. 5c and d).¹³ If the excimer species were $\text{Zn}^{\text{II}}(\text{hfac})_2(\text{PyBTM})_2$, I_{exc} should be much smaller than I_{mono} for **PyZn_5** and **PyZn_10**¹⁴ according to the first and second points above, but this would contradict the third point. Therefore, we concluded that the excimer emissive species in this system was not $\text{Zn}^{\text{II}}(\text{hfac})_2(\text{PyBTM})_2$, but the $\text{Zn}^{\text{II}}(\text{hfac})_2(\alpha\text{H-PyBTM})(\text{PyBTM})$ dimer. Considering the similarity between

emission behaviours of **PyZn_R** under a magnetic field and that of **PyBTM**-doped α H-**PyBTM**, a similar mechanism for the MFE was expected, where the magnetic field modulates the spin multiplicity changes of the dimer in both the ground and excited states (Fig. S8, ESI†).^{7,8}

In conclusion, the luminescent behaviours of **PyBTM**-substituted $\text{Zn}^{\text{II}}(\text{hfac})_2(\alpha\text{H-PyBTM})_2$ crystals, **PyZn_R**, depend on the radical concentration and external magnetic field. **PyZn_1** displayed emission from the monomer $\text{Zn}^{\text{II}}(\text{hfac})_2(\alpha\text{H-PyBTM})(\text{PyBTM})$ and this emission was not magnetic-field-sensitive. In contrast, **PyZn_5**, **PyZn_10**, and **PyZn_20** displayed both monomer and excimer emissions, which were modulated strongly by the magnetic field. These are the first-reported examples of excimer emission and magnetoluminescence in luminescent radical-coordinated metal complexes. Considering their emission properties and MFE behaviours, the excimer emissive species was identified not as $\text{Zn}^{\text{II}}(\text{hfac})_2(\text{PyBTM})_2$ but as the $\text{Zn}^{\text{II}}(\text{hfac})_2(\alpha\text{H-PyBTM})(\text{PyBTM})$ dimer. These results suggest the general nature of MFEs on the luminescence of radicals¹⁵ as well as the importance of the type of interaction between radicals. Because complexation could modulate the inter/intramolecular interaction of spins, the development of MFEs on luminescent radical-ligated complexes would be a promising strategy, and this research surely is an important step in developing new photofunctions based on the interplay between spin and luminescence.

The present study was supported by the JST CREST (Grant Number JPMJCR15F2) and JSPS KAKENHI (Grant Numbers JP20H02759, JP19K22197, JP17H04870, JP19H05460, and JP26220801). T. K. is grateful to the Iketani Science and Technology Foundation and the Kato Foundation for the Promotion of Science for financial support. S. K. acknowledges MERIT (Material Education program for the future leaders in Research, Industry, and Technology) in the MEXT Leading Graduate School Doctoral Program. Emission spectra measurements under a magnetic field were performed at the High Field Laboratory for Superconducting Materials, Institute for Materials Research, Tohoku University (Project No. 18H0018 and 19H0052). This work was partly supported by the Nanotechnology Platform Program (Molecule and Material Synthesis) of the MEXT, Japan.

Conflicts of interest

There are no conflicts to declare.

Notes and references

- (a) C. W. Tang, S. A. Vanslyke and C. H. Chen, *Appl. Phys. Lett.*, 1989, **65**, 3610–3616; (b) M. A. Baldo, D. F. O'Brien, Y. You, A. Shoustikov, S. Sibley, M. E. Thompson and S. R. Forrest, *Nature*, 1998, **395**, 151–154; (c) A. Endo, M. Ogasawara, A. Takahashi, D. Yokoyama, Y. Kato and C. Adachi, *Adv. Mater.*, 2009, **21**, 4802–4806; (d) H. Uoyama, K. Goushi, K. Shizu, H. Nomura and C. Adachi, *Nature*, 2012, **492**, 234–238.
- (a) E. D. Cosco, J. R. Caram, O. T. Bruns, D. Franke, R. A. Day, E. P. Farr, M. G. Bawendi and E. M. Sletten, *Angew. Chem., Int. Ed.*, 2017, **56**, 13126–13129; (b) A. L. Antaris, H. Chen, K. Cheng, Y. Sun, G. Hong, C. Qu, S. Diao, Z. Deng, X. Hu, B. Zhang, X. Zhang, O. K. Yaghi, Z. R. Alamparambil, X. Hong, Z. Cheng and H. Dai, *Nat. Mater.*, 2016, **15**, 235–242.
- (a) V. Gamero, D. Velasco, S. Latorre, F. López-Calahorra, E. Brillas and L. Juliá, *Tetrahedron Lett.*, 2006, **47**, 2305–2309; (b) A. Heckmann, S. Du, J. Pauli, M. Margraf, J. Ko, D. Stich, C. Lambert, I. Fischer and U. Resch-genger, *J. Phys. Chem. C*, 2009, **113**, 20958–20966.
- (a) X. Ai, E. W. Evans, S. Dong, A. J. Gillett, H. Guo, Y. Chen, T. J. H. Hele, R. H. Friend and F. Li, *Nature*, 2018, **563**, 536–540; (b) H. Guo, Q. Peng, X. K. Chen, Q. Gu, S. Dong, E. W. Evans, A. J. Gillett, X. Ai, M. Zhang, D. Credgington, V. Coropceanu, R. H. Friend, J. L. Brédas and F. Li, *Nat. Mater.*, 2019, **18**, 977–984; (c) Q. Peng, A. Obolda, M. Zhang and F. Li, *Angew. Chem., Int. Ed.*, 2015, **54**, 7091–7095; (d) A. Obolda, X. Ai, M. Zhang and F. Li, *ACS Appl. Mater. Interfaces*, 2016, **8**, 35472–35478; (e) Q. Gu, A. Abdurahman, R. H. Friend and F. Li, *J. Phys. Chem. Lett.*, 2020, **11**, 5638–5642; (f) A. Abdurahman, T. J. H. Hele, Q. Gu, J. Zhang, Q. Peng, M. Zhang, R. H. Friend, F. Li and E. W. Evans, *Nat. Mater.*, 2020, DOI: 10.1038/s41563-020-0705-9.
- (a) Y. Beldjoudi, M. Nascimento, Y. J. Cho, H. Yu, H. Aziz, D. Tonouchi, K. Eguchi, M. M. Matsushita, K. Awaga, I. O. Osorio-roman, C. P. Constantinides and J. M. Rawson, *J. Am. Chem. Soc.*, 2018, **140**, 6260–6270; (b) P. Mayorga Burrezo, V. G. Jiménez, D. Blasi, I. Ratera, A. G. Campaña and J. Veciana, *Angew. Chem., Int. Ed.*, 2019, **58**, 16282–16288; (c) P. Mayorga-Burrezo, V. G. Jiménez, D. Blasi, T. Parella, I. Ratera, A. G. Campaña and J. Veciana, *Chem. – Eur. J.*, 2020, **26**, 3776–3781; (d) K. An, G. Xie, S. Gong, Z. Chen, X. Zhou, F. Ni and C. Yang, *Sci. China: Chem.*, 2020, **63**, 1214–1220.
- (a) Y. Hattori, S. Kimura, T. Kusamoto, H. Maeda and H. Nishihara, *Chem. Commun.*, 2018, **54**, 615–618; (b) Y. Hattori, T. Kusamoto and H. Nishihara, *Angew. Chem., Int. Ed.*, 2014, **53**, 11845–11848; (c) Y. Hattori, T. Kusamoto and H. Nishihara, *Angew. Chem., Int. Ed.*, 2015, **54**, 3731–3734.
- S. Kimura, T. Kusamoto, S. Kimura, K. Kato, Y. Teki and H. Nishihara, *Angew. Chem., Int. Ed.*, 2018, **57**, 12711–12715.
- K. Kato, S. Kimura, T. Kusamoto, H. Nishihara and Y. Teki, *Angew. Chem., Int. Ed.*, 2019, **58**, 2606–2611.
- T. Kusamoto, Y. Hattori, A. Tanushi and H. Nishihara, *Inorg. Chem.*, 2015, **54**, 4186–4188.
- (a) Y. Hattori, T. Kusamoto, T. Sato and H. Nishihara, *Chem. Commun.*, 2016, **52**, 13393–13396; (b) Y. Ogino, T. Kusamoto, Y. Hattori, M. Shimada, M. Tsuchiya, Y. Yamanoi, E. Nishibori, K. Sugimoto and H. Nishihara, *Inorg. Chem.*, 2017, **56**, 3909–3915.
- D. Blasi, D. M. Nikolaidou, F. Terenziani, I. Ratera and J. Veciana, *Phys. Chem. Chem. Phys.*, 2017, **19**, 9313–9319.
- If $\text{Zn}^{\text{II}}(\text{hfac})_2(\text{PyBTM})_2$ was preferentially formed and the crystals consisted of a mixture of $\text{Zn}^{\text{II}}(\text{hfac})_2(\alpha\text{H-PyBTM})_2$ and $\text{Zn}^{\text{II}}(\text{hfac})_2(\text{PyBTM})_2$, the excimer emission could not emerge as the radical concentrations increased. Therefore, these results confirmed that $\alpha\text{H-PyBTM}$ in the $\text{Zn}^{\text{II}}(\text{hfac})_2(\alpha\text{H-PyBTM})_2$ crystals was randomly substituted with **PyBTM**.
- The contributions of the emission components mean the peak areas of emission bands and were estimated by Gaussian deconvolutions. The details are shown in the ESI†.
- The exciton transfer from monomer emissive states to excimer emissive states can be negligible because emission decays of **PyZn_10** at 900 nm, where excimer emission components were dominant, did not show slow rising time (Fig. S6d, ESI†).
- Similarity in the magnetoluminescence behaviours between the previous reports and the present system indicates that the MFE observed is not compound-specific but general for luminescent doublet molecules.